Single Conjugate Adaptive Optics for METIS

Thomas Bertram[a], Olivier Absil[b], Peter Bizenberger[a], Wolfgang Brandner[a], Florian Briegel[a], Faustine Cantalloube[a], Brunella Carlomagno[b], María Concepción Cárdenas Vázquez[a], Markus Feldt[a], Adrian M. Glauser[c], Thomas Henning[a], Stefan Hippler[a], Armin Huber[a], Norma Hurtado[d], Matthew A. Kenworthy[e], Martin Kulas[a], Lars Mohr[a], Vianak Naranjo[a], Philip Neureuther[f], Andreas Obereder[g], Ralf-Rainer Rohloff[a], Silvia Scheithauer[a], Iuliia Shatokhina[h], Remko Stuik[e], and Roy van Boekel[a]

[a]Max-Planck-Institut für Astronomie, Königstuhl 17, 69117 Heidelberg, Germany
[b]STAR Institute, Université de Liège, 19c allée du Six Août, bât B5c, 4000 Liège, Belgium
[c]Institute for Particle Physics and Astrophysics, ETH Zürich, Wolfgang-Pauli-Str. 27, 8093 Zürich, Switzerland
[d]ASTRON, Oude Hoogeveensedijk 4, 7991 PD Dwingeloo The Netherlands
[e]Leiden Observatory, PO Box 9500, 2300 RA Leiden, The Netherlands
[f]Institute for System Dynamics, University of Stuttgart, Waldburgstraße 17/19, 70563 Stuttgart, Germany
[g]MathConsult GmbH, Altembergerstraße 69, 4040 Linz, Austria
[h]Industrial Mathematics Institute, Johannes Kepler University Linz, Altembergerstraße 69, 4040 Linz, Austria

ABSTRACT

METIS is the Mid-infrared Extremely large Telescope Imager and Spectrograph, one of the first generation instruments of ESO's 39m ELT. All scientific observing modes of METIS require adaptive optics (AO) correction close to the diffraction limit. Demanding constraints are introduced by the foreseen coronagraphy modes, which require highest angular resolution and PSF stability. Further design drivers for METIS and its AO system are imposed by the wavelength regime: observations in the thermal infrared require an elaborate thermal, baffling and masking concept.

METIS will be equipped with a Single-Conjugate Adaptive Optics (SCAO) system. An integral part of the instrument is the SCAO module. It will host a pyramid type wavefront sensor, operating in the near-IR and located inside the cryogenic environment of the METIS instrument. The wavefront control loop as well as secondary control tasks will be realized within the AO Control System, as part of the instrument. Its main actuators will be the adaptive quaternary mirror and the field stabilization mirror of the ELT.

In this paper we report on the phase B design work for the METIS SCAO system; the opto-mechanical design of the SCAO module as well as the control loop concepts and analyses. Simulations were carried out to address a number of important aspects, such as the impact of the fragmented pupil of the ELT on wavefront reconstruction. The trade-off that led to the decision for a pyramid wavefront sensor will be explained, as well as the additional control tasks such as pupil stabilization and compensation of non-common path aberrations.

Keywords: SCAO, METIS, ELT, NIR wavefront sensor, pyramid wavefront sensor

1. INTRODUCTION

The Mid-infrared ELT Imager and Spectrograph (METIS)[1] belongs the first generation of science instruments to be used with the Extremely Large Telescope (ELT). Its realization is a joint undertaking of nine institutes from eight European countries and ESO. The project is currently in its preliminary design phase. Once operational,

Send correspondence to T. Bertram (E-mail: bertram@mpia.de, Telephone: +49 6221 528-441)

METIS will provide an unprecedented performance in terms of angular resolution and contrast in the mid-infrared wavelength regime. Observation capabilities include imaging and low/medium resolution spectroscopy at L/M band (2.9 µm – 5.3 µm) and N/Q band (7.0 µm – 19.0 µm), high resolution integral field spectroscopy at L/M band, and coronagraphy for High Contrast Imaging (HCI).

Ground based observing in the thermal infrared requires a number of measures to deal with the background. These measures include fast observing and calibration strategies[2] such as chopping in the science channel and fast detector readout, a mostly cryogenic environment for the components in the optical path and an elaborate masking and baffling concept.

All observing modes for METIS require Adaptive Optics to facilitate the needed temporal and spatial correction of the incoming wavefront. METIS will be equipped with a classical SCAO system, which is well suited for the high contrast science cases. Here the targets of interest are observed in the vicinity of bright and compact on-axis reference objects. The ultimate solution to overcome the limitations of an SCAO system in sky coverage while providing good performance would be the implementation of an additional Laser Tomography Adaptive Optics system for METIS. For programmatic reasons, however, such a development is not on the horizon. Therefore, an alternate solution, using only a single Laser Guide Star (SLAO), is being investigated.

The SCAO system for METIS consists of a number of entities, distributed across the instrument and telescope domain. Figure 1 lists hardware and control entities relevant to SCAO. The control scheme is outlined in Figure 2: An SCAO module with a Near-Infrared pyramid wavefront sensor (WFS)[3,4] detects wavefront aberrations. The Instrument Real-Time Computer (RTC) will process the WFS data and calculate correction signals, which are sent via the Central Control System (CCS) of the ELT to the main actuators for wavefront control: the deformable mirror M4 and the field stabilization mirror M5 of the ELT.

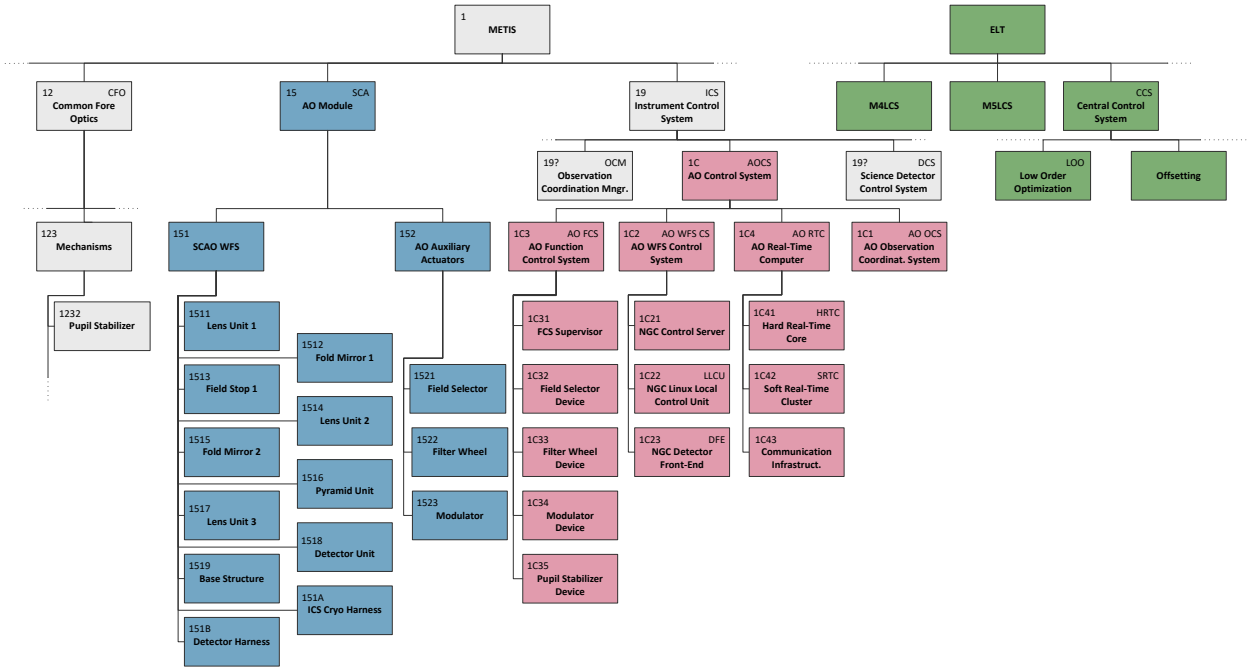

Figure 1. Partial breakdown of METIS and ELT identifying the main entities relevant to SCAO. Different colors are used to highlight different branches: blue – SCAO module, red – AO control system, green – ELT. The numbers are the corresponding codes in the METIS Product Breakdown Structure.

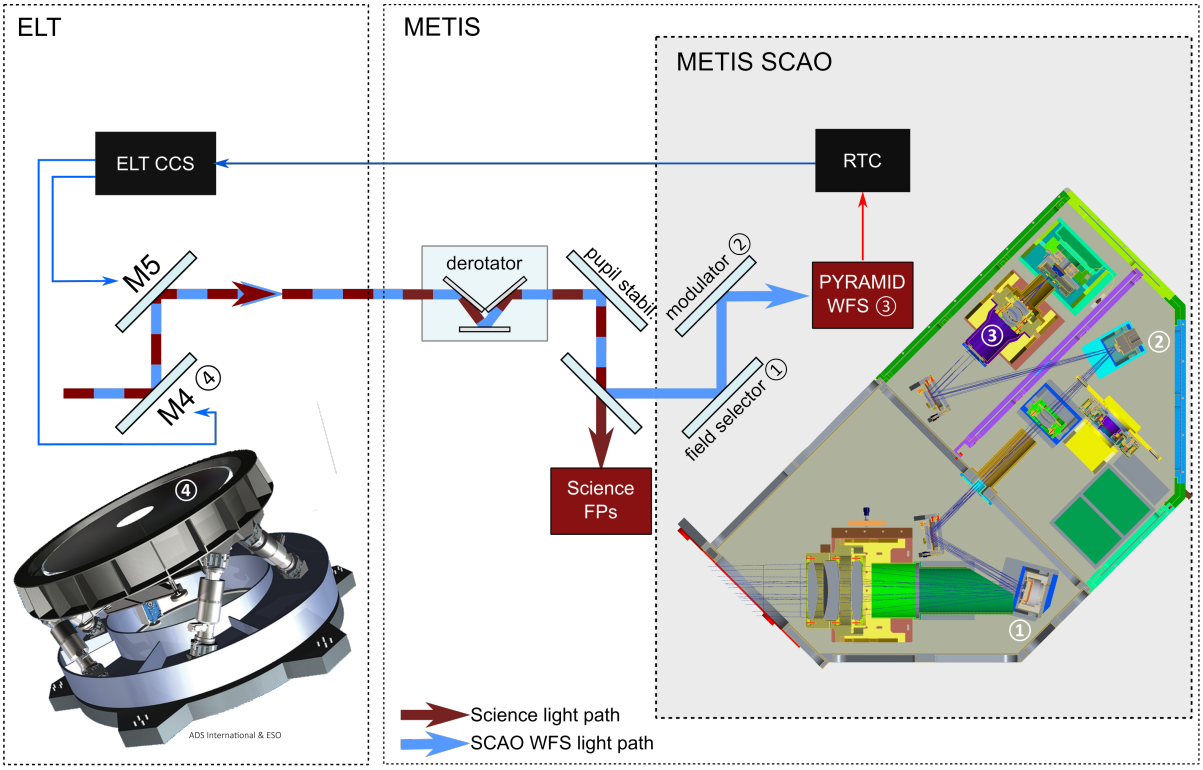

Figure 2. Control scheme for METIS SCAO. The propagates through telescope and instrument. The Near Infrared part of the light (blue) is directed to the SCAO module, which uses a couple of field steering actuators (① and ②, see Section 5) and a pyramid WFS to detect wavefront aberrations. The wavefront is reconstructed and correction signals are calculated by the instrument RTC, which sends the correction signals via the Central Control System of the ELT to the actuators of the wavefront control loop: the deformable mirror M4 and the field stabilization mirror M5.

2. SPECIFICATIONS

The required performance of the SCAO system in terms of mean residual wavefront error and resulting Strehl ratio is expressed in the top level requirements for METIS. A minimum Strehl ratio of 60% (goal: 80%) at the reference wavelength of 3.7µm and 93% (goal: 95%) at 10µm shall be delivered for a natural guide star with m_K=10 mag and a median V-band seeing of 0.65". High Contrast Imaging[5] imposes further requirements on the SCAO performance: METIS shall deliver a 5σ contrast at L-band of $3 \cdot 10^{-5}$ (goal: 10^{-6}) at a distance of $5\lambda/D$ (goal: $2\lambda/D$), which relates to the efficiency of the wavefront correction especially at low spatial frequencies.

On instrument level, a number of functions have been assigned to the SCAO system:

- Wavefront Control
- Pupil stabilization
- Correction of non-common path aberrations and differential tip/tilt between WFS and science path.

In addition, a number of SCAO internal functions will have to be realized:

- Field selection for the acquisition of the natural guide star.
- Management of the registration between M4 and the WFS, including pupil rotation.
- Optimization of control loop parameters.

Table 1. Key design parameters for METIS SCAO

Wavelength range [a]	1.45 µm – 2.45 µm
Field Selector FoV	∅ 27”
Selected FoV	∅ 2”
Optical wavefront decomposition	pyramid
Pupil sampling	0.5m
Number of subapertures	77×77
Detector type	Leonardo Saphira eAPD
Detector geometry	256×320
Pixel per subaperture	1 [b]
Pixel size	24 µm
Frame rate	100 Hz – 1 kHz
Readout mode	Fowler-N
ADC for WFS	No [c]
Field Selector	Yes
Modulator	Yes
Operating temperature	70 K
Command degrees of freedom	5316 +2
Command rate	$\leq$ 1 kHz

[a] can be reduced by different bandpass filters
[b] per quadrant
[c] common Atmospheric Dispersion Corrector (ADC); possibly restriction to K-band

Table 1 lists key parameters for design of the METIS SCAO hardware as well as the control loops. Additional parameters on atmospheric conditions and telescope performance to be considered for the analysis and design have been provided by ESO.

3. WAVEFRONT SENSOR TRADE-OFF STUDY

Early 2017 a trade-off study was carried out between a Shack-Hartmann type and a Pyramid type WFS, with the intention to consolidate the choice for the SCAO WFS of METIS and to identify, if an additional cophasing device would be needed. The previous baseline to use a Shack-Hartmann WFS was mainly based on a complexity argument. A more thorough analysis was required which considered the wavefront sensing performance for different scenarios and, more specifically, the performance when having to deal with the fragmentation of the ELT pupil, as well as technical and programmatic aspects.

Fragmentation of the ELT pupil The obscuration introduced by the telescope spiders dissects the pupil in six fragments with gaps wider than a 0.5m subaperture. Wavefront reconstruction must not treat these fragments individually; a solution has to be found that spans the entire aperture.[6,7] In a modal basis that is defined across the entire aperture, differential piston here is defined as mode which offsets the surface of an individual pupil fragment with respect to the surface of the other fragments. The differential piston aberrations between pupil fragments can be introduced by the AO loop itself, as a result of missing information or wrong interpretation of the WFS signals – this case is referred to as *island effect*. Also possible is a physical origin (discontinuities in the incoming phase, seen in open loop), e.g. in the case of the *low wind effect*.[8] It is detrimental for both Strehl ratio (cf. Figure 3) and contrast (cf. Figure 4).

The Shack-Hartmann WFS, being a slope sensor, is insensitive to phase discontinuities introduced by the island effect, especially if the separating gap is wider than the size of a subaperture. On the contrary, the Pyramid WFS is, within limits, sensitive to phase discontinuities.[9,10]

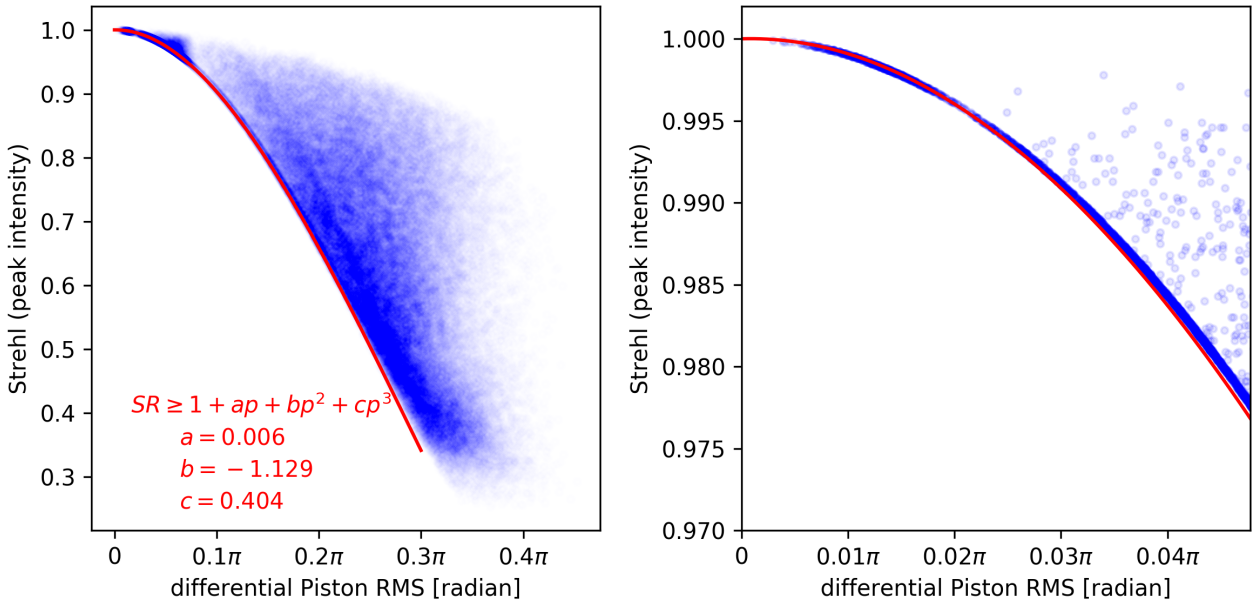

Figure 3. Differential Piston vs. Strehl ratio. The differential piston is randomly introduced for all six fragments in the METIS pupil. The RMS differential piston in the aperture is plotted against the peak intensity in the monochromatic, flux-normalized PSF. A lower limit to the resulting Strehl ratio can be expressed as 3rd degree polynomial. The density distribution indicates that, for any given RMS differential piston, the achieved Strehl ratio is most likely at or near the lower limit. Note: to better sample the lower limit at low R differential piston additional samples were added in the range [0–0.1π].

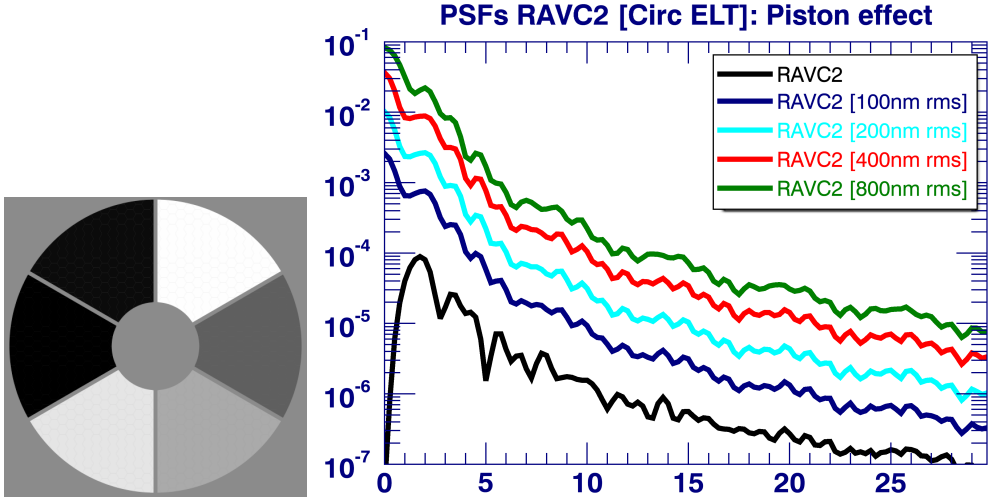

Figure 4. Contrast achievable with the ring apodized vortex coronagraph under the influence of variable RMS differential piston. Contrast is plotted against angular distance. A circular aperture with a thin spider is considered.

Performance In a number of end-to-end simulations, the performance of different configurations of Shack-Hartmann and Pyramid wavefront sensors was analyzed for different seeing conditions, guide star magnitudes and loop frequencies. The scope of these simulations was to compare the different WFS types under the same conditions, and not to derive the overall performance of METIS SCAO. It has to be noted that we were not able find a working solution for the island effect in the case of a Shack-Hartmann WFS and did not consider the fragmentation of the ELT pupil in the Shack-Hartmann configurations.

As expected, the Pyramid WFS shows the best performance in terms of Strehl Ratio, especially at the faint

end. But also in terms of residual image motion and contrast the pyramid WFS shows a better performance.

Technical and Programmatic Considerations One of the aspects to be considered is the detector format and the availability of large infrared detector arrays suitable for Adaptive Optics. A Shack-Hartmann WFS for METIS would require a detector array that exceeds the dimensions of the existing 256×320 pixel SAPHIRA eAPD. Such a development is ongoing, but the low technical readiness of such a to be developed device adds a programmatic risk to the project. On the other hand, the need for a modulator that is capable to operate in a cryogenic environment also imposes a risk.

The trade-off study resulted in the decision to change the baseline in favor of a pyramid type WFS. An additional co-phasing device was deemed as not necessary.

4. SIMULATIONS

A number of analyses are performed to assess the performance of METIS SCAO and the impact of various degrading effects. Examples for topical analyses include, but are not limited to, the residual wavefront error in terms of Strehl ratio (Figure 5), the impact of non-common path aberrations on the SCAO performance (Figure 6) or the impact of imperfect correction of atmospheric differential refraction by the Atmospheric Dispersion Corrector (ADC) in the common path.

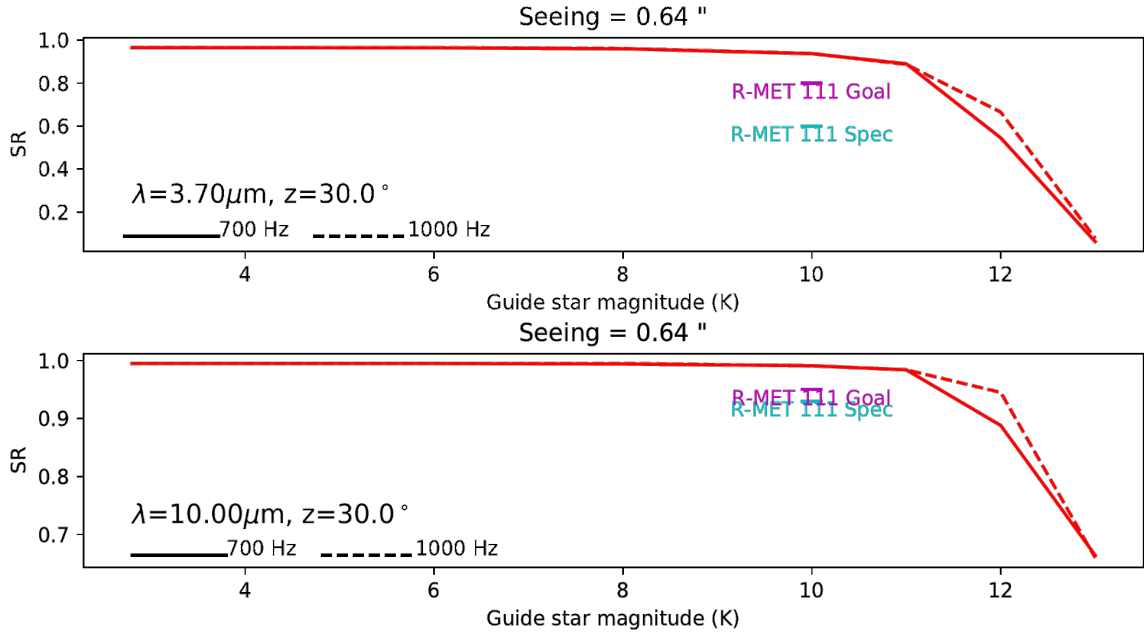

Figure 5. Simulated performance of METIS SCAO in terms of Strehl ratio (SR) as function of the guide star magnitude. The results are preliminary and refer to the Strehl ratio at 3.7 µm and 10.0 µm at the position of the WFS. Additional performance degrading effects have to be considered to determine the expected performance for METIS, such as non-common path aberrations or wind shake. Also shown are the performance requirements and goals (SR at m_K=10 mag).

The analyses are being carried out with the help of several end-to-end simulation tools: YAO,[11] COMPASS[12] and OCTOPUS.[13] Furthermore, synthetic modeling is applied to help to establish the error budget with regard to the contrast performance of the instrument. The simulations play also an important role in the dimensioning of the SCAO system and the development of key components of the wavefront control loop for METIS SCAO, like the wavefront reconstruction algorithm[14] or the controller.

Due to its importance for the scientific success of METIS, emphasis has been placed in the last months on the analysis of the achievable contrast after post-processing. For this analysis, residual phase screens produced by

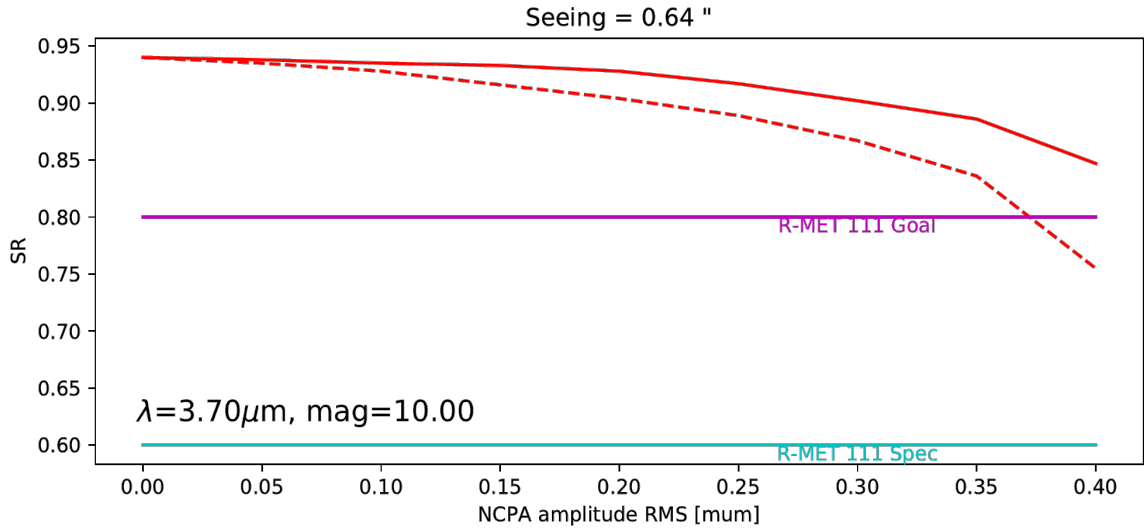

Figure 6. Simulated performance of the METIS SCAO in terms of Strehl ratio (SR) as function of the amount of non-common path aberrations (NCPA). The aim of this analysis is to determine the amount of NCPA which can still be tolerated when offsetting Pyramid WFS signals to compensate for NCPA in the science path.

optimized SCAO end-to-end simulations are propagated through a vortex simulation. This is work in progress and cannot be concluded at the time of writing this status update.

5. WAVEFRONT SENSING WITHIN METIS

The opto-mechanical design of METIS is outlined in Figure 7.

Like most other subsystems, the SCAO module resides inside the METIS cryostat. Its location in the optical path[15] is the result of a number of design considerations:

- The pick-off mirror for SCAO has to be at cryogenic temperatures to limit background radiation.
- The pick-off mirror is located as much downstream in the instrument as possible. This reduces the non-common path wavefront error between the WFS and the science focal planes.
- The chopper is in the non-common path. The field on the WFS is not affected by chopping offsets.
- The derotator is in the common path and its effects on the lateral field and pupil position is seen by the WFS.

Figure 8 shows the opto-mechanical design of the SCAO module, the subsystem of METIS that contains the pyramid WFS and auxiliary actuators.

The *Field Selector* is a unit at the entrance of the SCAO Module. Its task is to choose the field to be directed towards the WFS, which allows to select the natural guide star from anywhere in the scientific field of view. It is realized as an actively controlled tip/tilt mirror located in the first pupil plane of the SCAO Module. A challenge for the actuator is the combination of high angular resolution over a large travel range at cryogenic operating conditions. The setting requires about $1.6{\cdot}10^5$ resolution elements over a travel range of 6°.

A second tip/tilt mirror in the optical train is the *Modulator*. It will be used to modulate the light over the four facets of the pyramid, thus allowing to trade linear range and sensitivity of the pyramid WFS. A sinusoidal tip-tilt motion of the mirror will cause the image of the natural guide star to move along a circular path around the tip of the pyramid. The frequency with which the circular path is commanded has to be synchronized with the readout frequency of the detector (up to 1 kHz) and the radius of the circular path needs to be adjustable

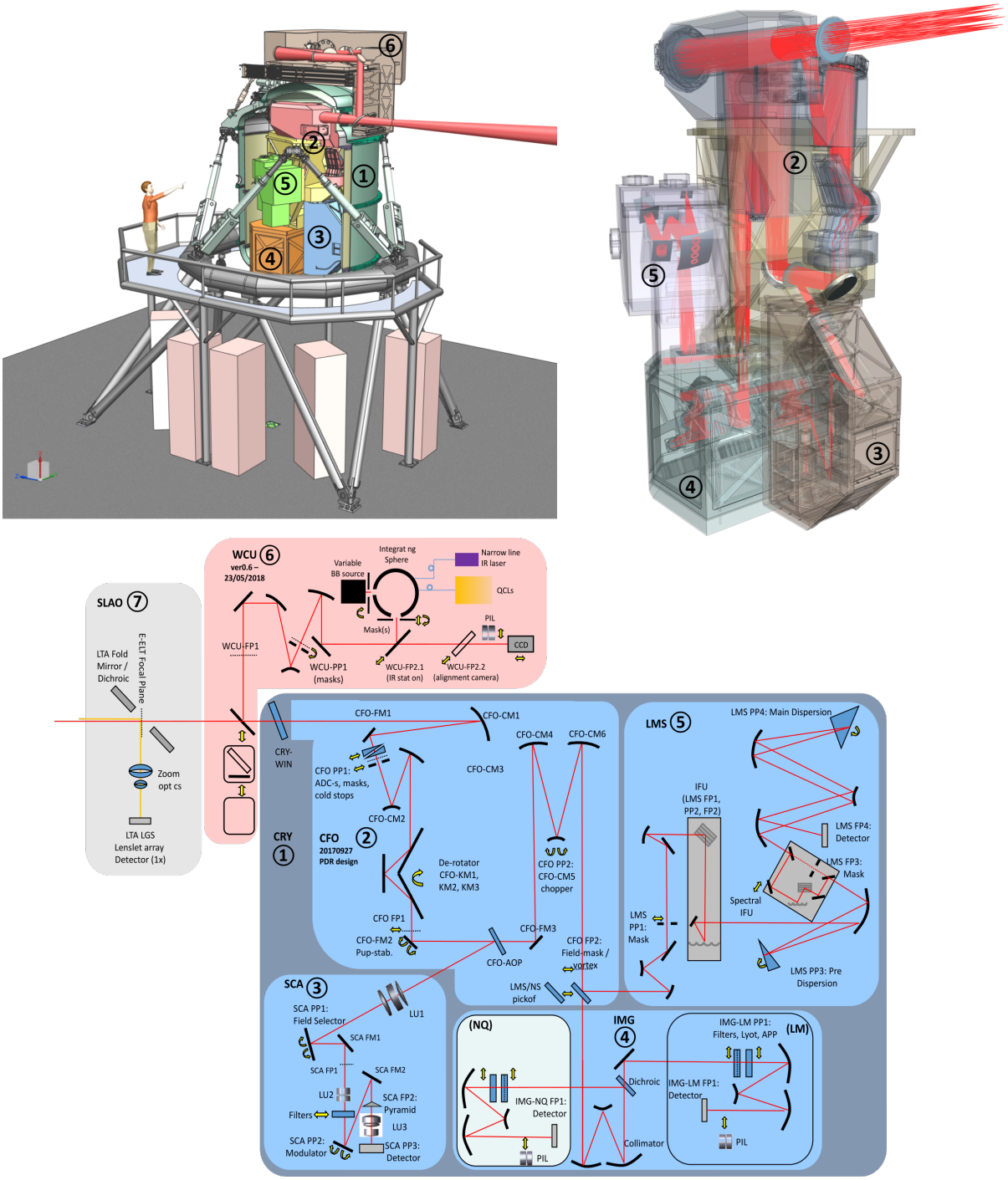

Figure 7. Opto-mechanical design of METIS. The instrument consists of a number of subsystems, most of which are located inside the Cryostat ①. The Central Fore Optics ② provides the necessary optical interfaces for the other optical subsystems. It contains a derotator and a pupil stabilization mechanism in the common path as well as a chopping mechanism in the science path of the instrument. The near infrared part of the light is then directed towards the SCAO module ③. Longer wave bands are transmitted towards the Imager ④ and the LM Spectrograph ⑤. The sources of a Warm Calibration Unit ⑥ can be folded into the optical path at the entrance of the instrument. A single Laser Guide Star system ⑦ is being investigated.

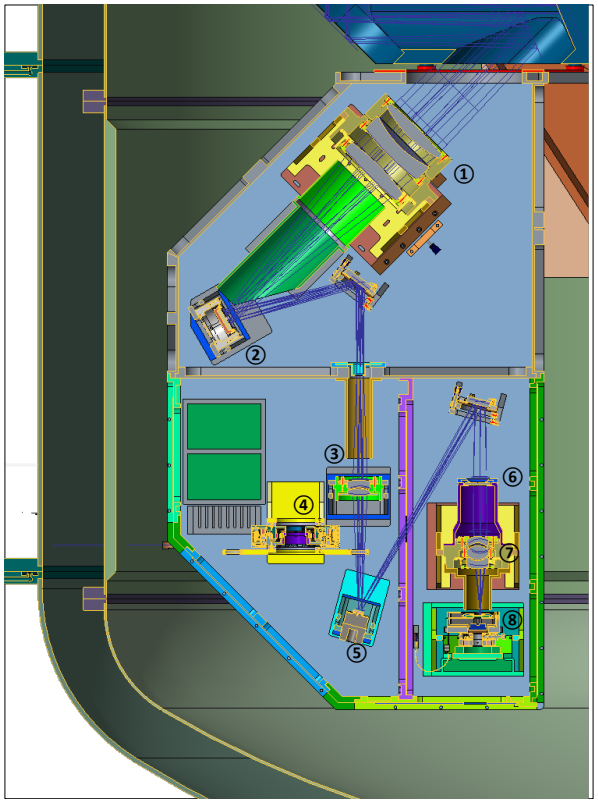

Figure 8. Opto-mechanical design of the SCAO module. A first pupil image is formed on the Field Selector ② by lens unit 1 ① and a second pupil image on the Modulator ⑤ by lens unit 2 ③. Both mirrors allow to control the position of the field on the pyramid ⑥. Only a small field is propagated downstream of the Field Selector. A filter wheel ④ allows to adjust the pass bands and gray filters in case of very bright reference targets. The reimaging lens group 3 ⑦ produces the four images of M4 on the Saphira detector ⑦ as seen through the pyramid.

up to 10 λ/D. Again, the realization of such an actuator for cryogenic operating conditions is a challenge. First feasibility studies have been carried out for both cryogenic tip/tilt actuators by potential suppliers. These studies included design concepts. The first study supports the feasibility of such devices, for which prototypes will have to be built next. A second study carried out by another potential supplier is ongoing.

A filter wheel will allow to select bandpass and neutral density filters to avoid saturation on the brightest targets. Field stops are introduced in the focal plane downstream of the Field Selector and at the pyramid itself. The WFS signal will be obtained with a *Saphira detector*[16] and the readout electronics provided by ESO.

6. AO CONTROL SYSTEM

The AO Control System is, as part of the Instrument Control System of METIS, responsible for the AO wavefront correction and a number of related secondary control tasks. A crucial component within the AO Control System is the Real-Time Computer, which will consist of a Hard Real-Time Core (HRTC) for the time critical computations of the wavefront control loop and a Soft Real-Time Cluster (SRTC) for supporting less time critical computations that rely on AO telemetry data. The framework in which the AO Control System has to be realized will be defined by ESO. The METIS SCAO team is now tasked with the identification of a suitable HRTC solution. Kulas et al.[17] report on the RTC concept for METIS and the evaluation of a manycore CPU based RTC.

In addition to the main wavefront control loop, a number of additional loops will be realized within the AO Control System. Figure 9 outlines the control schemes for the wavefront control loop, the pupil stabilization loop and the loop for the compensation of non-common path aberrations.

Wavefront Control

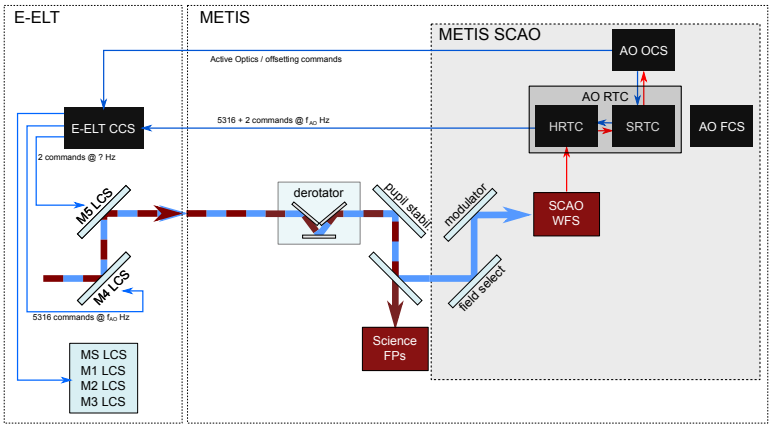

Pupil Stabilization

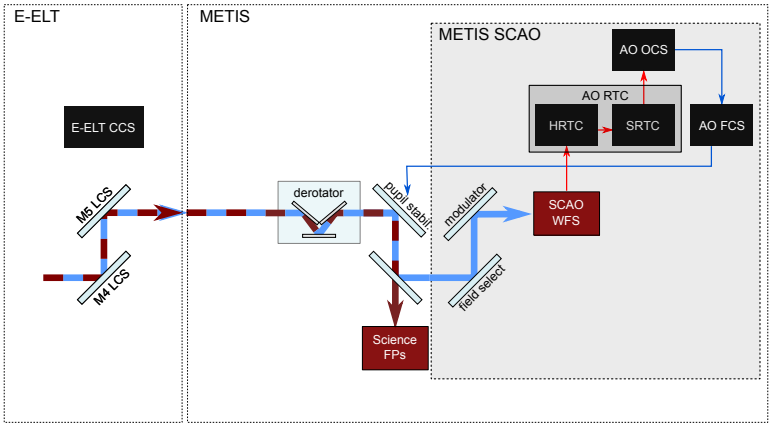

NCPA Compensation

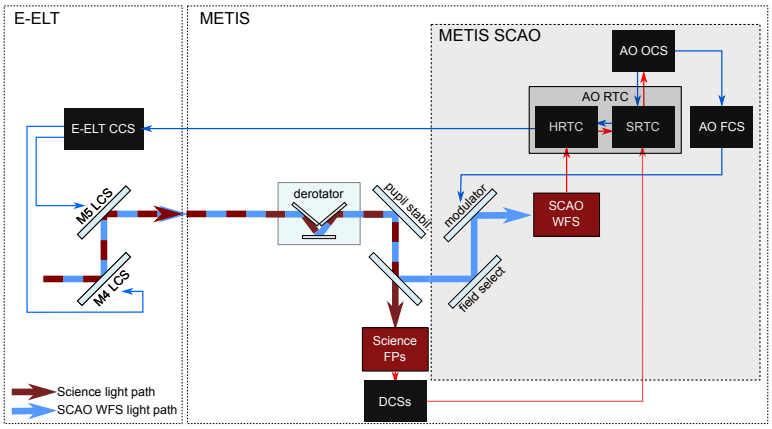

Figure 9. METIS SCAO control schemes for wavefront control, pupil stabilization and NCPA compensation. The components inside the gray box are part of METIS SCAO. Red arrows indicate measurement signal flow, blue arrows command flow. Red boxes represent sensors, black boxes represent control instances. The HRTC within AO RTC is responsible for the core wavefront control loop, data products that rely on WFS telemetry are computed in the SRTC. Secondary control tasks, such as registration management, modulation, and field selection will be performed outside of the AO RTC. For NCPA compensation, data from the Science Detectors will be used as well as AO telemetry data.

REFERENCES

[1] Brandl, B. R., Feldt, M., Garcia, P., Glasse, A., Guedel, . M., Labadie, L., Pantin, E., Schmid, H. M., van Winckel, . H., Bettonvil, F., van Boekel, R., Glauser, A. M., Hurtado, N. ., and Quanz, S. P., "Status of the mid-infrared E-ELT imager and spectrograph METIS," *SPIE* **10702**, 10702–66 (2018).

[2] Burtscher, L., van Boekel, R., Brandl, B., Baccichet, N., Labadie, L., Hurtado, N., Muzic, K., Jellema, W., Zeilinger, W., Käufl, H.-U., Kausch, W., Pantin, E., Vandenbussche, B., Glasse, A., Kenworthy, M., Absil, O., Bettonvil, F., Glauser, A., Lynn, J., and Meisner, J., "The calibration scheme for ELT/METIS," *SPIE* **10704**, 10704–97 (2018).

[3] Ragazzoni, R., "Pupil plane wavefront sensing with an oscillating prism," *Journal of Modern Optics* **43**, 289–293 (Feb. 1996).

[4] Ragazzoni, R. and Farinato, J., "Sensitivity of a pyramidic Wave Front sensor in closed loop Adaptive Optics," *A&A* **350**, L23–L26 (Oct. 1999).

[5] Kenworthy, M. A., Absil, O., Carlomagno, B., Snik, F., Agócs, T., Por, E. H., and Brandl, B. R., "A review of high contrast imaging modes for METIS," *SPIE* **10702**, 10702–369 (2018).

[6] Obereder, A., Raffetseder, S., Hutterer, V., and Shatokhina, I., "Dealing with Spiders on ELTs: using a Pyramid WFS to overcome residual piston effects," *SPIE* **10703**, 10703–50 (2018).

[7] Schwartz, N., Sauvage, J.-F., Correia, C. M., Neichel, B., Fusco, T., Quiros-Pacheco, F., Dohlen, K., ElHadi, K., Agapito, G., Thatte, N., and Clarke, C., "Analysis and mitigation of pupil discontinuities on adaptive optics performance," *SPIE* **10703**, 10703–75 (2018).

[8] Sauvage, J.-F., Fusco, T., Guesalaga, A., Wizinowitch, P., O'Neal, J., N'Diaye, M., and Vigan, A., "Low Wind Effect, the main limitation of the SPHERE instrument," in [*Adaptive Optics for Extremely Large Telescopes 4 – Conference Proceedings*], (2015).

[9] Esposito, S. and Devaney, N., "Segmented telescopes co-phasing using Pyramid Sensor," in [*European Southern Observatory Conference and Workshop Proceedings*], Vernet, E., Ragazzoni, R., Esposito, S., and Hubin, N., eds., *ESO Conference and Workshop Proceedings* **58**, 161 (2002).

[10] Pinna, E., Quiros-Pacheco, F., Esposito, S., Puglisi, A., and Stefanini, P., "The Pyramid Phasing Sensor (PYPS)," in [*Ground-based and Airborne Telescopes II*], *SPIE* **7012**, 70123D (July 2008).

[11] Rigaut, F. and Van Dam, M., "Simulating Astronomical Adaptive Optics Systems Using Yao," in [*Proceedings of the Third AO4ELT Conference*], Esposito, S. and Fini, L., eds., 18 (Dec. 2013).

[12] Gratadour, D., Ferreira, F., Sevin, A., Doucet, N., Clénet, Y., Gendron, E., Lainé, M., Vidal, F., Brulé, J., Puech, M., Vérinaud, C., and Carlotti, A., "COMPASS: status update and long term development plan," in [*Adaptive Optics Systems V*], *SPIE* **9909**, 990971 (July 2016).

[13] Montilla, I., Béchet, C., Lelouarn, M., Correia, C., Tallon, M., Reyes, M., and Thiébaut, É., "Comparison of Reconstruction and Control algorithms on the ESO end-to- end simulator OCTOPUS," in [*Adaptative Optics for Extremely Large Telescopes*], 03002 (Jan. 2010).

[14] Hutterer, V., Shatokhina, I., Obereder, A., and Ramlau, R., "Wavefront reconstruction for ELT-sized telescopes with pyramid wavefront sensors ," *SPIE* **10703**, 10703–154 (2018).

[15] Agócs, T., Jellema, W., van den Born, J., ter Horst, R., Bizenberger, P., Cárdenas Vázquez, C., Todd, S., Baccichet, N., and Straubmeier, C., "End to end optical design and wavefront error simulation of METIS," *SPIE* **10702**, 10702–353 (2018).

[16] Finger, G., Baker, I., Alvarez, D., Ives, D., Mehrgan, L., Meyer, M., Stegmeier, J., and Weller, H. J., "SAPHIRA detector for infrared wavefront sensing," *SPIE* **9148**, 914817 (Aug. 2014).

[17] Kulas, M., Bertram, T., and Briegel, F., "METIS AO RTC Concept," *SPIE* **10707**, 10707–87 (2018).